AIAA JOURNAL
Vol. 31, No. 10, October 1993

Observations of Liquid Jets Injected into a Highly Accelerated Supersonic Boundary Layer

Arthur W. Johnson* and K. R. Sreenivasan†
Yale University, New Haven, Connecticut 06520

Experiments were conducted to observe the cross-sectional structure and streamwise growth of round transverse liquid jets injected into a highly accelerated boundary layer in supersonic flow. The accompanying shock structure was also visualized. In one case, a round jet of acetone was injected into a fully turbulent Mach 2.5 boundary layer that was subsequently accelerated and partially laminarized through a sharp Prandtl-Meyer expansion corner. In the second case, a jet was injected into the laminarized Mach 3.2 boundary layer downstream of the expansion corner at the same jet-to-freestream momentum ratio. The jet and shock structure in both cases were visualized using schlieren optics. Wall-flow patterns were visualized using paints. It was found that the lateral spreading of jets injected downstream of the expansion fan was augmented close to the wall and had a cross-sectional structure significantly different from that of the jet injected upstream: the upstream jet spreads rapidly at the expansion corner in both the lateral and vertical directions.

Nomenclature

d = diameter of jet orifice
M = Mach number
P = pressure
Re = Reynolds number
St = Stokes number, t_p/t_f
T = temperature
t_f = time scale for host flow
t_p = time scale for the deceleration of acetone droplets
U = mean velocity
U^+ = $U_{vd}(\rho_w/\tau_w)^{1/2}$
u' = root-mean-square of velocity fluctuations
y = normal distance from the wall
y^+ = yU^+/ν
δ = boundary-layer thickness (y at $0.99U_\infty$)
δ^* = displacement thickness
θ = momentum thickness
ν = kinematic viscosity
ρ = density
τ = shear stress

Subscripts
vd = Van Driest transformed quantity
w = wall conditions
0 = stagnation condition
∞ = freestream conditions

Introduction

TRANSVERSE injection of jets in supersonic crossflow are of continuing interest in areas such as the combustion of fuel/air mixtures in scramjet combustors and for thrust-vectoring devices on aircraft.[1-3] In many cases, the jet is injected into a boundary layer highly accelerated by a rounded or sharp convex corner. It is well known that the structure of accelerated turbulent boundary layers is significantly distorted and may "laminarize" if the pressure gradient is strong enough.[4-8] Characteristics of highly accelerated boundary layers, such as larger near-wall gradients of Mach number and velocity, thickening of the sublayer, and lower turbulence intensities, are likely to influence the mixing and the complicated three-dimensional flowfield due to the interaction of the transverse jet and the boundary layer.

Significant features of the flowfield produced by the interaction of a jet and a supersonic crossflow are shown in Fig. 1. Upstream of the jet, the flow separates, and consequently a "separation shock" leading to a three-dimensional bow shock over the jet is created. Horseshoe vortices are formed just upstream of the jet in the separated flow as described by Shang et al.,[9] and the associated counter-rotating vortices are convected downstream adjacent to the jet. The number, strength, and size of the horseshoe vortices depend on a variety of factors such as the upstream shock configuration, jet pressure, and velocity. In studies by Shang et al. for a gaseous jet injected into a hypersonic crossflow, up to four vortices were found numerically in the upstream separation region. The cross section of the jet near the nozzle (Fig. 2) is deformed to an elliptical or kidney shape,[10] whereas the interaction of the flow with the jet column creates a pair of counter-rotating vortices as modeled by Heister et al.[11] The three-dimensional bow shock upstream of the jet is, as discussed by Kumar et al.,[2] a significant source of mean and fluctuating vorticity.

It is of interest to examine whether the structure and development of a jet injected downstream of a Prandtl-Meyer expansion corner would be affected by the distorted velocity profile and reduced turbulence intensity characteristic of the highly accelerated boundary layer. It would also be of interest to compare the jet spread and other flow characteristics in this case with those of a jet injected upstream of the Prandtl-

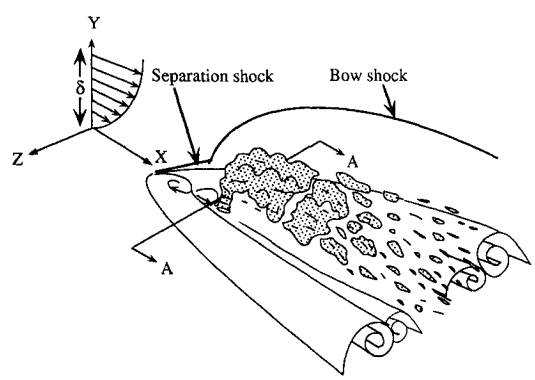

Fig. 1 Isometric sketch of liquid jet in supersonic crossflow with associated separated flow. Vortices are not to scale.

Received July 19, 1992; revision received Nov. 10, 1992; accepted for publication Nov. 29, 1992.

*Graduate Research Assistant, Department of Mechanical Engineering. Member AIAA.
†Professor of Mechanical Engineering. Member AIAA.

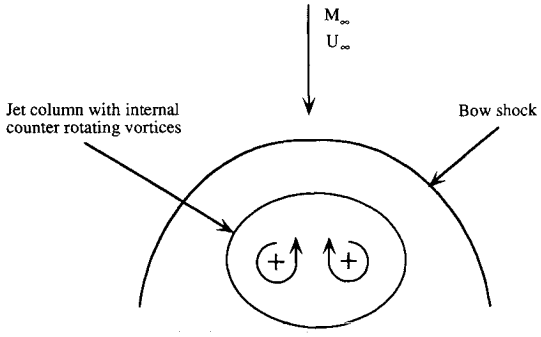

Fig. 2 Cross-sectional structure near the jet exit, section A-A of Fig. 1.

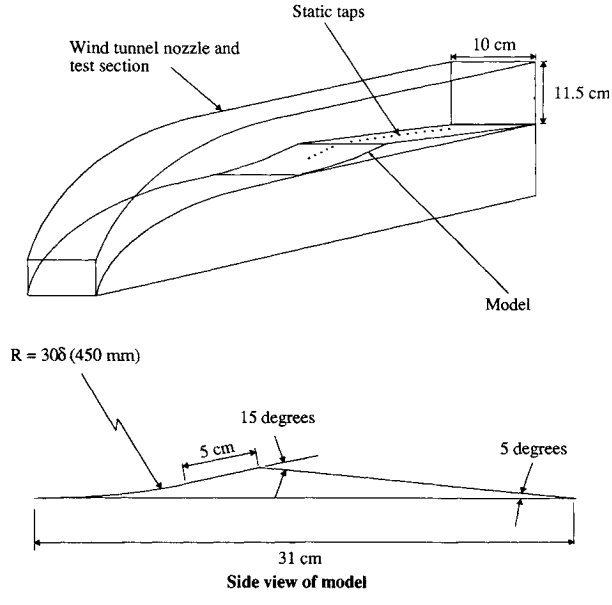

Fig. 3 Test section and model.

Meyer expansion. Jets injected upstream mix better in the vertical direction because of the divergence of streamlines through the Prandtl-Meyer expansion and in the lateral direction because of the amplification of streamwise vortices.

The intent of this study is to observe and compare the streamwise growth, shock structure, and cross-sectional structure of round transverse liquid jets interacting with an accelerated supersonic boundary layer. Two cases are considered. The first considers an acetone jet injected into a laminarized Mach 3.2 boundary layer just downstream of an expansion corner. The second case considers a jet injected into the fully turbulent Mach 2.5 boundary layer just upstream of the Prandtl-Meyer expansion and its subsequent evolution as it negotiates the expansion and mixes far downstream. The jet-to-freestream momentum ratio in both cases was set to 0.92. The jet developments in the two cases are compared by visualizing the shock structure, cross-sectional flow structure, and lateral and vertical growth of the jets. Patterns of jet contact at the wall were also determined. Some interpretation of the observed differences in the two cases is provided.

Experiment

Experiments were conducted in a variable Mach number blowdown supersonic wind tunnel with a cross-sectional area of 10×11.5 cm. A turbulent boundary layer developed on the floor of the wind tunnel and negotiated a single cornered wedge model with curved forebody as shown in Fig. 3. The radius of curvature of the forebody was $R/\delta = 30$. The boundary layer subsequently developed on the straight part of the wedge before encountering a 15-deg expansion corner. Static taps of diameter 0.68 mm were drilled along the center of the model spaced 3.17 mm apart. These taps also served as ports for jet injection. Jets were injected from a pressurized reservoir, and the flow rate was calibrated and controlled by the upstream pressure setting. The wind tunnel was operated with a stagnation pressure of 4.9×10^5 Pa and average stagnation temperature of 291 K. Wall conditions were nearly adiabatic. The approximate run time of the wind tunnel was 30 s, whereas the times required to reach a steady state for the wind tunnel and injection apparatus are on the order of 10 and 0.25 s, respectively. All data were taken within a 15-s window of steady operating conditions.

Properties of the mean flow without injection were measured using static taps and flattened pitot probes. The pitot probe dimensions were set within limits determined experimentally by Allen[12] so that corrections to the measurements were not required. Stagnation temperature and pressure were measured from the settling chamber upstream of the test section.

Turbulent quantities were measured using normal 5-μm-diam tungsten hot wires with an etched length of 0.7 mm. The frequency response of the wires was tuned approximately flat up to 250 kHz. This corresponds to $5U_\infty/\delta$ which, according to Kistler,[13] resolves the energy-containing motion of the boundary-layer fluctuations. The overheat ratio of the constant temperature DISA anemometer at room temperature was set to 0.9. The output of the anemometer was separated into a mean and fluctuating component using two signal conditioners to amplify and prefilter the data. The fluctuating component of the signal was high passed at 10 Hz and low passed at 250 kHz. The hot-wire data, as well as the pressure and temperature measurements, were recorded using a concurrent data acquisition system whose upper limit on the sampling rate was 1 MHz.

Calibration and interpretation of hot-wire signals were based on the methods discussed by Smits and Muck.[14] Density fluctuations were separated from the signal using the so-called "strong Reynolds analogy" developed by Morkovin[15] that assumes an adiabatic flow with negligible pressure and total temperature fluctuations. The formulation leads to the following relationship that describes the proportionality of velocity fluctuations and fluctuations of mass flux $(\rho u)'$ measured by the hot wire:

$$\frac{u'}{U} = [1 + (\gamma - 1)M^2]^{-1}\frac{(\rho u)'}{\rho U}$$

Acetone was chosen as the fluid for injection. Because of the relatively high boiling point and low surface tension of acetone, it atomizes to very small droplet sizes when sheared by the crossflow. Studies by Smith[16] have shown that the droplet sizes of an acetone fog in flows comparable to the one studied here are on the order of 3 μm in diameter. Although the droplets are not expected to follow the flow near the wall when negotiating the Prandtl-Meyer corner, Smith[16] has found that acetone droplets follow large-scale turbulent structures adequately.

Acetone was injected at two locations into the mean flow. The first location was 19 mm ($28d$) before the expansion corner, whereas in the second experiment the acetone was injected 50 mm ($74d$) after the expansion corner. At the downstream injection location, the pressure gradient was zero and the flow uniform. The jet-to-freestream momentum ratio in both experiments was approximately 0.92. Although it would be desirable to use a higher momentum ratio to simulate practical circumstances, our facility prevented reliable operation at higher pressures. The momentum ratio used provides enough penetration height to observe the salient features of the jet structure.

Spark and continuous schlieren optics were used to ascertain shock patterns, flow structures, and turbulent regions of both the basic flow and the flow with injection. The duration of the spark schlieren was approximately 20 ns. The schlieren

images were recorded on a video camera and digitized using a PC-based video editing system.

The cross-sectional structures of the jets were visualized using Mie scattering with laser optics to determine their "edges." The optical configuration is shown in Fig. 4. A 1-mW helium-neon laser beam was converted to a sheet of thickness nearly 0.25 mm and passed through the jet in cross-flow. The laser sheet was oriented at positions perpendicular to the wall of the model and the direction of the mean flow. The scattered laser light was recorded on a video camera. The images were then digitized using a frame grabber with a 647×480 square pixel array. Considering the system as a whole, the resolution consists of a 540×280 pixel array covering a 27×27-mm area for the laser images. The average signal-to-noise ratio was on the order of 30. From the images, the edges of the cross sections were determined visually and marked on photographs. As a check, the edges were redetermined using a pixel thresholding method. A histogram of pixel intensities of the digitized images was obtained. The peak of the histogram is the average pixel value of the background, and the pixel intensity defining the boundary was the threshold above which the slope of the histogram began to asymptote to zero (for details, see Prasad and Sreenivasan[17]). The coordinates of these edges were then measured using appropriate scales and recorded.

The surface of the wedge model was coated with black paint in some experiments to obtain a qualitative picture of jet contact at the wall. The paint is wiped away wherever fresh acetone contacts the wall.

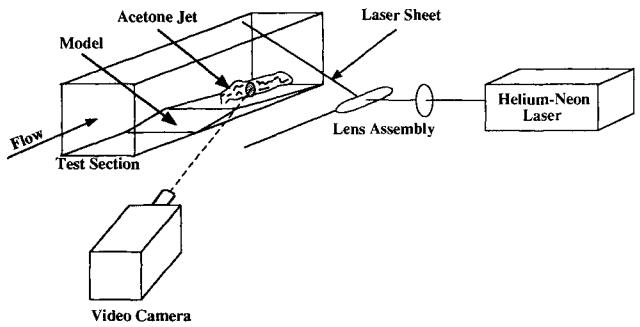

Fig. 4 Optical arrangement for the visualization of jet cross sections. The beam from a 1-mW helium-neon laser passes through a spherical lens focused on the test section and converted to a sheet of light with thickness of order ~ 0.25 mm. Mie scattered light from the acetone droplets of the jet is recorded by a video camera focused on the laser sheet at the jet cross section.

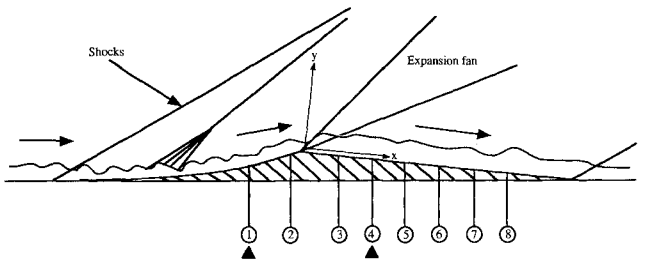

	x (mm)	M_∞	U_∞(m/s)	δ^*(mm)	θ (mm)	Re_θ
1	-19	2.5	565.4	3.2	0.75	37,000
2	-5	2.5	569.4	3.1	0.75	37,200
3	25	3.13	616.3	3.1	0.66	21,900
4	50	3.2	625.9	4.4	0.79	25,900
5	75	3.2	625.3	4.7	0.83	27,100
6	100	3.2	625.9	4.7	0.83	27,200
7	125	3.2	625.6	4.9	0.86	28,100
8	150	3.2	625.5	5.4	0.94	30,700

Fig. 5 Properties of the mean flow: ▲, injection point locations.

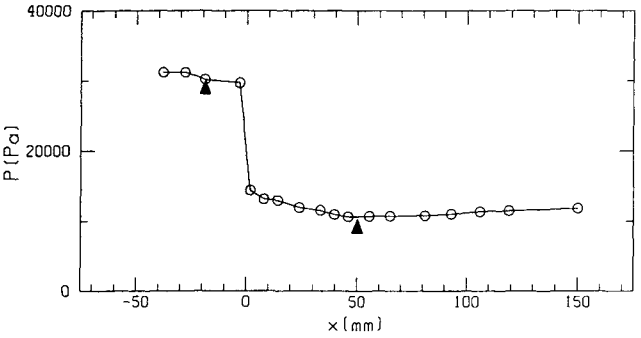

Fig. 6 Static pressure distribution. Origin is at the expansion corner: ▲ marks injection points at $x = -19$ and 50 mm.

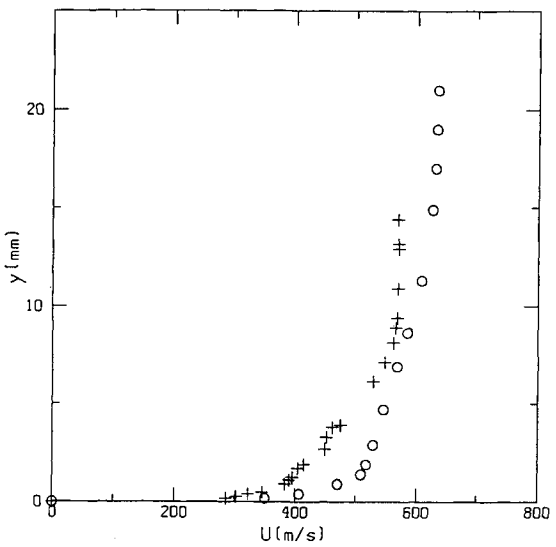

Fig. 7 Velocity profiles of the basic flow at points of injection: +, 19 mm upstream of the corner; ○, 50 mm downstream of the corner.

Results and Discussion

Properties of the mean flow as measured by the static pressure tap and pitot probe measures are shown in Fig. 5. The mean velocity was converted to the incompressible form using the Van Driest transformation[18]:

$$U(y)_{vd} = \int_0^y \left(\frac{\rho}{\rho_w}\right)^{1/2} dU$$

The static pressure along the centerline of the wedge is shown in Fig. 6. The Mach 2.5 turbulent boundary layer upstream of the corner was accelerated to Mach 3.2 by the favorable pressure gradient at the Prandtl-Meyer expansion fan. Note that this 28% increase in Mach number translates to only a 10% increase in freestream velocity. The ratio of the pressure drop to upstream wall shear stress was on the order of 100. This meets the criteria for laminarization of turbulent boundary layers.[5] Here, the pressure drop was ascertained from the static pressure measurements, whereas the wall shear stress upstream of the corner was estimated using the best log-law fit to the mean velocity profile data. The structure of the boundary-layer velocity profiles at the chosen points of jet injection is shown in Fig. 7. The velocity profile becomes distorted and more full as it negotiates the expansion. When plotted in wall variables (Fig. 8), the distortion can be seen clearly in the downstream velocity profile; furthermore, there

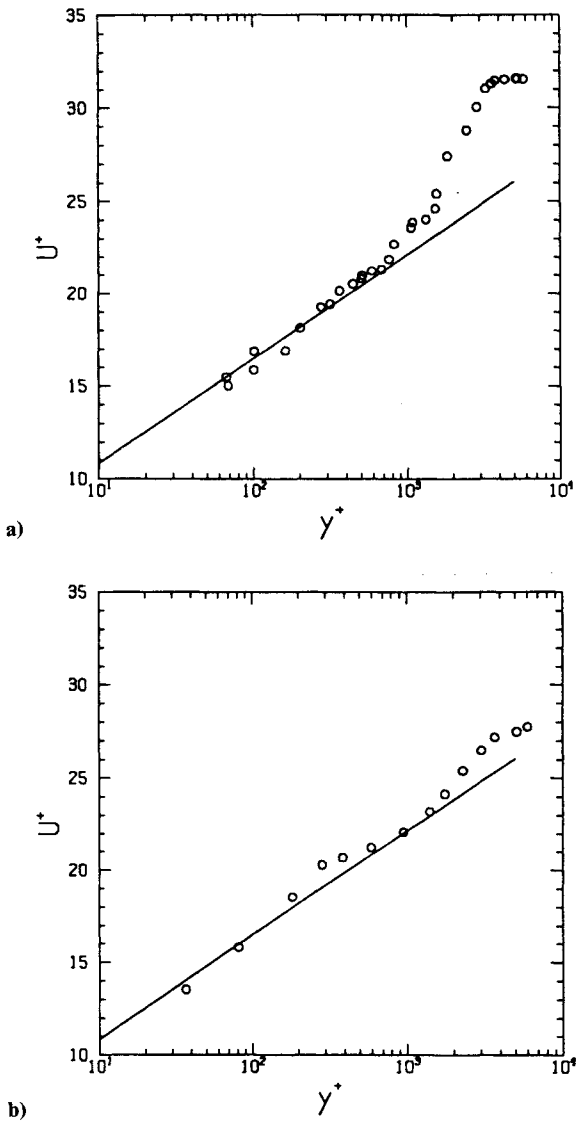

Fig. 8 Van Driest transformed velocity profiles at points of injection: a) 19 mm upstream of expansion corner and b) 50 mm downstream of expansion corner. Lines: $U^+ = 2.45\ \ln(y^+) + 5.2$.

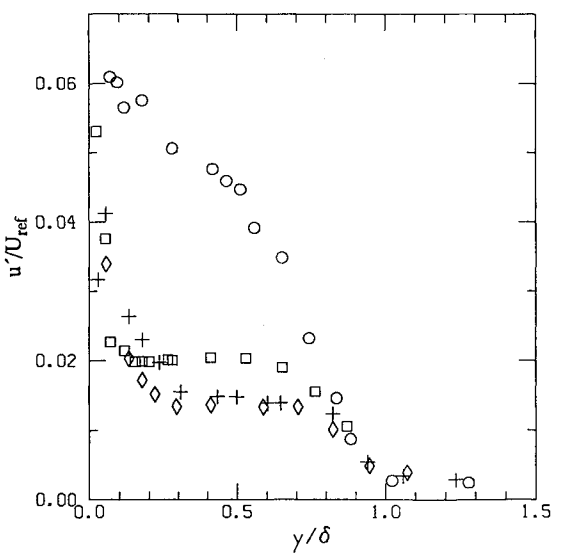

Fig. 9 Velocity fluctuation intensity through the expansion and at downstream locations. The reference velocity, $U_{ref} = 569$ m/s, is the freestream value at $x = -19$ mm; ○, $x = -19$ mm; □, $x = 50$ mm; ◇, $x = 100$ mm; +, $x = 150$ mm.

is a large reduction in the wake component due to the acceleration at the expansion corner.[4]

Hot-wire measures of the longitudinal velocity fluctuations show a significant reduction of up to 66% in intensity through the acceleration (Fig. 9). As the accelerated boundary layer develops downstream of the expansion, new turbulence is produced below $y/\delta = 0.1$ and slowly grows into regions away from the wall. The turbulent fluctuations above $y/\delta = 0.1$ decay slowly. It should be noted that the upstream boundary layer is recovering from a compression over a large radius of curvature. Yet the upstream turbulence level, when normalized as $(\bar{\rho}u'^2/\tau_w)^{1/2}$, is only slightly over the range measured in equilibrium turbulent boundary layers in supersonic flows[6] and maintains a similar structure. Such an observation is consistent with findings by Jayaram et al.,[19] who show that the turbulent structure for compressible boundary layers encountering mild concave curvature is not significantly altered.

Visualizations of the flowfields using spark and continuous schlieren optics are shown in Figs. 10a–10f. The basic flowfield without injection, Figs. 10a and 10d, has shocks from the leading edge and curved wall of the forebody of the wedge model. Downstream of the expansion fan at the corner, the development of a new laminar inner layer is visible at the wall. As expected, the bow shock and recompression shock of the jets in the two injection cases are different. The bow shock in front of the upstream jet (Figs. 10b and 10e) is more detached than that of the downstream jet (Figs. 10c and 10f) because it is injected into a lower Mach number flow. The recompression shock of the upstream jet is also farther away from the bow shock than that for the downstream jet. The separation shocks of the flows are not clearly visible with the present optics. Yet it is expected that the relatively full velocity profile (and Mach number profile) of the downstream flow (Fig. 7) will produce significantly different wave configurations upstream of the two jets. Although the positions of jet-associated shocks are discernible in Figs. 10, to facilitate easy reading, it seemed useful to mark the shock shapes explicitly. This is done in Fig. 11. The recompression shock of the upstream jet is not included because of its lack of definition in the schlieren photographs.

Because the mean flow is accelerated through the expansion corner, there are regions where the acetone droplets will not follow the mean streamlines. The acetone of the upstream jet does not appear to follow the flow near the wall as it negotiates the Prandtl-Meyer fan as shown in Figs. 10b and 10e. Close to the wall, the acceleration is most rapid and the Stokes number defined by $St = t_p/t_f$ is much greater than unity. However, it appears from Figs. 10b and 10e that the bulk of the jet flows roughly parallel to the wall and the edge of the boundary layer.

From Figs. 10b and 10e it can be seen that downstream of the expansion the upstream jet has a significant variation of acetone concentration and is convoluted by the remnant turbulence. The vertical spread of the jet is apparently not significant downstream of the expansion corner. These observations suggest that the upstream jet and associated separated flow have succeeded in preserving enough turbulence intensity through the expansion to allow significant large-scale mixing. It is possible that streamwise vortices produced by the upstream jet are amplified by the acceleration. Figures 10c and 10f indicate that the jet injected downstream of the expansion remains relatively smooth and of high concentration until nearly 80 jet diameters downstream. Here its edges become more convoluted and the jet grows significantly in the vertical direction. This growth is accompanied by significant dilution near the wall, and it appears that the jet is "lifting." Such a trend is most likely the result of the jet augmenting the natural retransition of the laminarized boundary layer to a fully turbulent state.[7]

Visualizations of regions where jet contact at the wall occurred are shown in Figs. 12a and 12b for the downstream and upstream cases, respectively. The wall was coated with a water-based paint, and the paint was wiped away wherever fresh

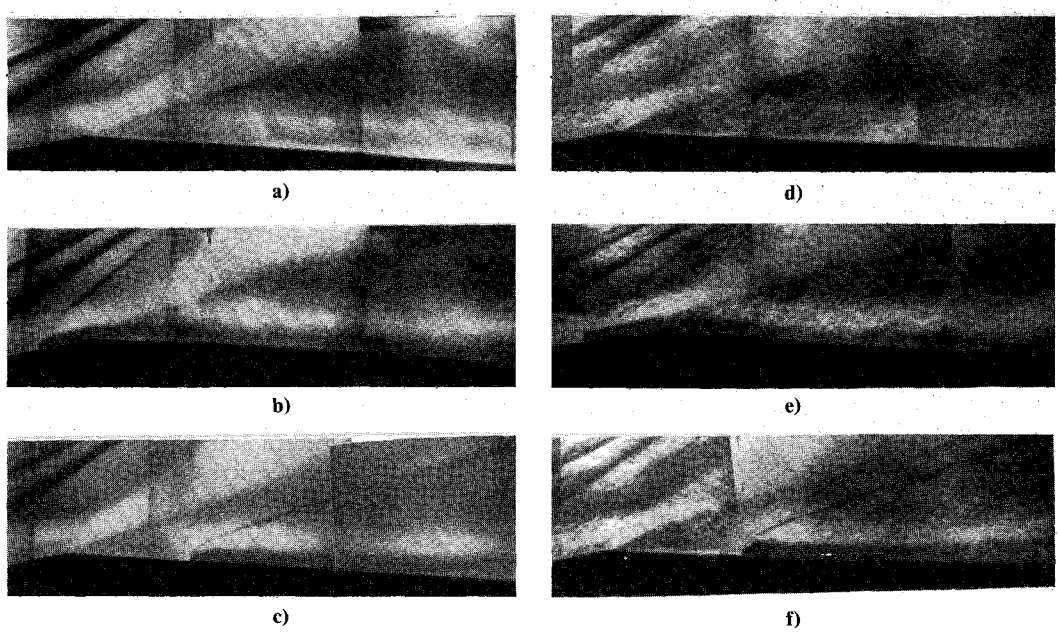

Fig. 10 Visualizations of the basic flow with the jet injection: a–c) time-averaged schlieren and d–f) spark schlieren. Each photograph is a composite of several photographs.

acetone contacted the wall. In the numerous operations of the wind tunnel with acetone injection, there was little variability in the wall patterns observed here. The extent of paint removed at the wall by the downstream jet compared with the upstream jet is greater in the lateral direction. Fingerlike patterns are found both just downstream of the downstream jet and just after the expansion corner for the upstream jet. It is believed that these regions mark separation zones where, as in oil flow visualizations, there is fluid accumulation in regions of separation. Such areas may also mark regions separating adjacent counter-rotating vortices produced in the separated flow. The extent of acetone contact at the wall upstream of the jets gives an indication of the length of the separation zone or upstream transport of jet fluid in each case. It was observed that the separation zone of the upstream jet extended 2.6 diameters upstream of the jet orifice, whereas this length for the downstream case was about 4.7 diameters. Studies by Zubkov and Glagolev[20] have shown that the length of the separation zone for gaseous jets injected into supersonic turbulent flows increases with boundary-layer thickness but decreases with Mach number. In this case, the downstream boundary layer is 50% thicker than the upstream turbulent boundary layer, has a higher Mach number and a lower sonic line, and is laminar-like instead of fully turbulent. Hence, it is apparent that the laminar-like characteristics and larger scale of the downstream boundary layer are sufficient to counter the effects of lower Mach number and lower sonic line, causing the flow to separate farther upstream for the downstream jet.

Measurements of the edges of the jet cross sections visualized using laser scattering at various downstream locations are shown in Fig. 13. Here, a three-dimensional perspective of the development of each flow shows that there is a significant difference in the shapes, growth, and relative sizes of the mean cross sections of the upstream and downstream jets. The downstream jet is significantly expanded in the spanwise direction close to the wall. The upstream jet is similar in size to the downstream jet until it encounters the Prandtl-Meyer corner; subsequently, it expands significantly in both the lateral and vertical directions.

The near-wall cross-sectional structure of the downstream jet is different from that of the jet injected upstream. Figure 14 is a plot of the edges of the jet cross sections visualized by the scattered laser light at $x/d = 28$ from their respective

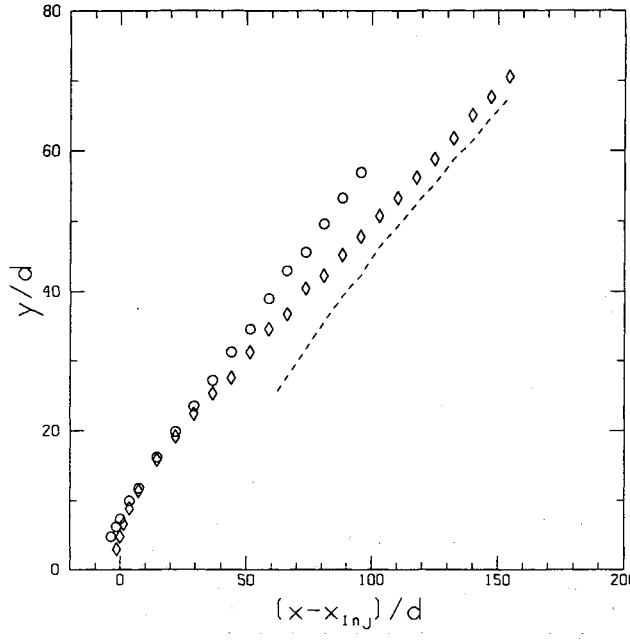

Fig. 11 Shock structure associated with the jets in crossflow: ○, bow shock of jet injected at $x_{inj} = -19$ mm upstream of the expansion corner; ◇, bow shock of jet injected $x_{inj} = 50$ mm downstream of the expansion. Dashed line marks recompression shock of downstream jet. Jet diameter $d = 0.68$ mm.

points of injection. Measurements of the jet edges from pixel thresholding are included for comparison and are seen not to be significantly different from edges determined visually. The height and shape of the jets are similar everywhere at this location except at regions below $y = 1$ mm. Below $y = 1$ mm, the lateral dimension of the downstream jet is twice as large as that of the upstream jet. It should be explicitly stated that the precise similarity coordinate for the jet spread is unlikely to be just the nozzle diameter. The purpose of Fig. 14 is chiefly to display qualitative differences in structure between jets injected into different crossflow conditions.

The enhanced spanwise transport of near-wall fluid in the downstream jet is believed to be largely the result of transport

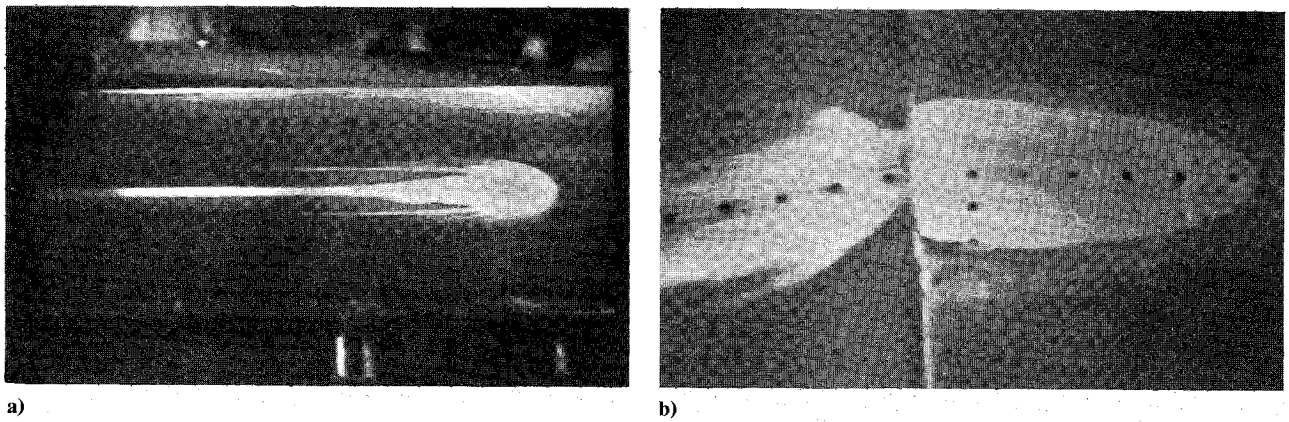

Fig. 12 Regions of jet contact at the wall. The wall was coated with a water-based paint that was wiped away when in contact with the acetone jet: a) injection location 50 mm downstream of the expansion corner and b) injection location 19 mm before the expansion corner. Flow direction is from right to left.

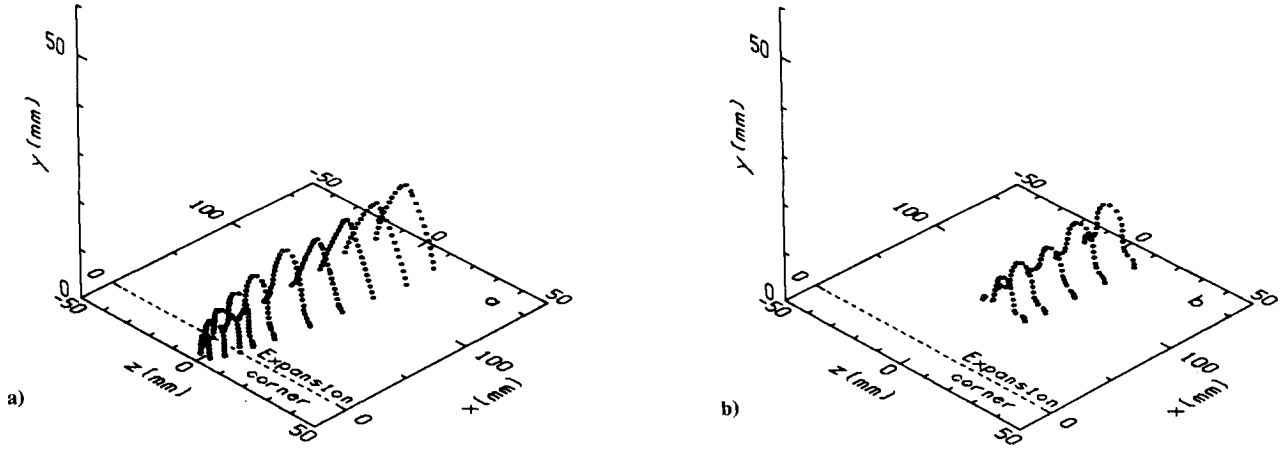

Fig. 13 Perspective view of the edges of the jet cross sections: a) jet injected 19 mm upstream of the expansion corner and b) jet injected 50 mm downstream of the expansion corner.

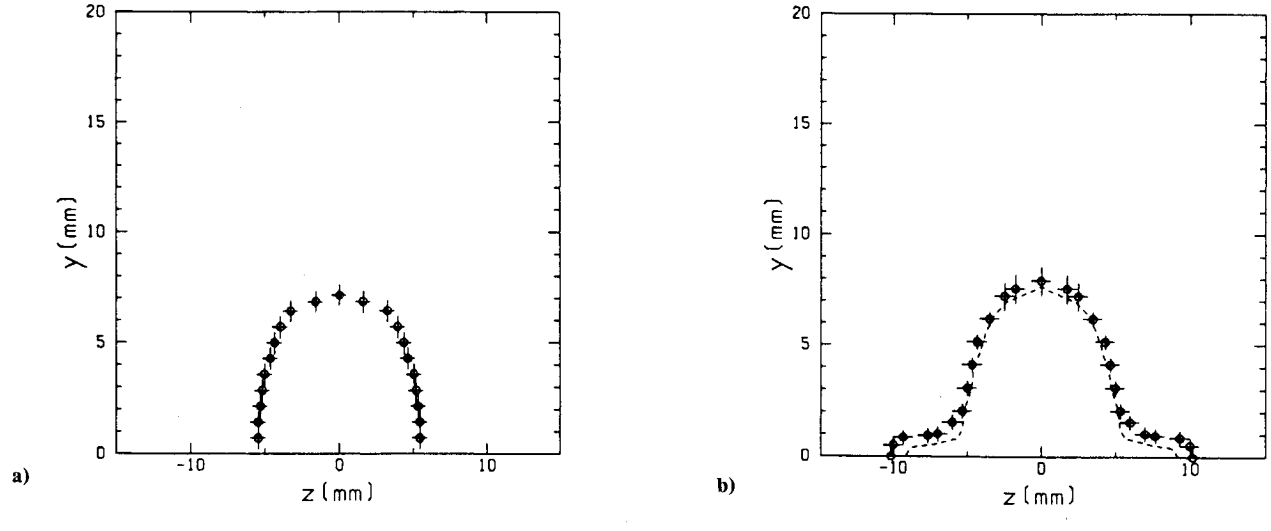

Fig. 14 Cross sections of the jets at $x/d = 28$ from points of injection: a) point of injection at $x/d = 28$ upstream of the expansion corner and b) point of injection $x/d = 73$ downstream of the expansion corner. Dashed line indicates measurements using pixel thresholding to mark edges of the cross section.

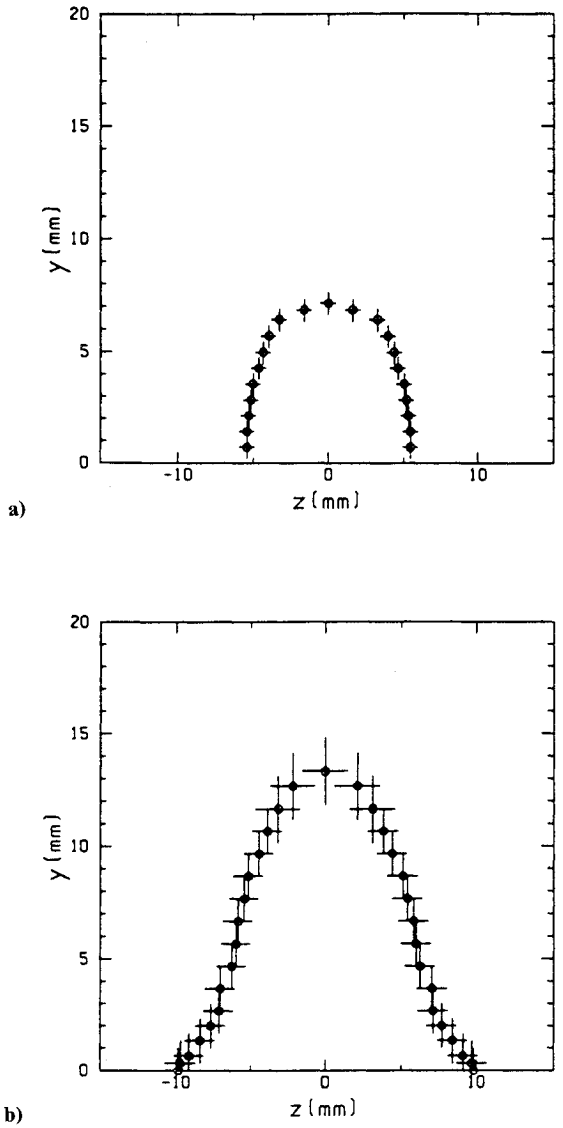

Fig. 15 Cross sections of the upstream jet before and after the expansion corner: a) 19 mm before the expansion corner and b) 50 mm after the expansion.

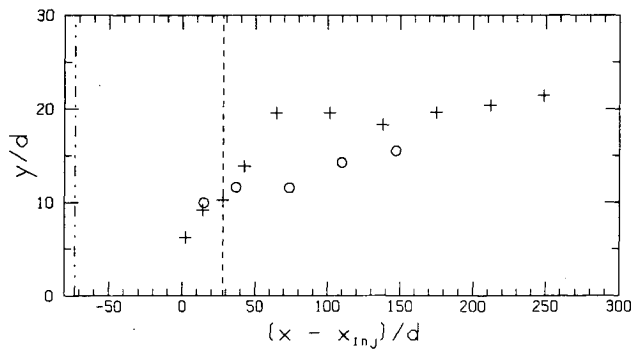

Fig. 16 Streamwise growth of the jets in crossflow: +, injection point x_{inj} = 19 mm before the expansion corner; o, injection point x_{inj} = 50 mm downstream of the corner; — - - —, expansion corner location relative to downstream jet; - - -, expansion corner location relative to upstream jet. Jet orifice diameter d = 0.68 mm.

by the horseshoe vortices created in the separated flow and convected downstream adjacent to the jet. Studies by Hung and Buning[21] for supersonic flows over blunt fins have shown that upstream horseshoe vortices are inviscid dominated and that their size and shape are affected by the upstream shock configuration. The observations of the boundary-layer velocity profiles in Fig. 7 indicate that the near-wall velocities (and Mach numbers) in the downstream boundary layer are greater, which in turn would strengthen spanwise vorticity in these regions and alter the shape of the upstream shocks. Wall patterns in Fig. 12 indicate that the length of the separation zone in front of the downstream jet is greater than that in the upstream case. Thus, it can be inferred that both the scale and strength of the horseshoe vortices in the downstream jet are significantly larger than those of the upstream jet.

It should also be noted that the differences in vertical penetration and lateral growth of the jets may be affected by the differences in freestream Mach numbers. Calculations by Li and Karagozian[22] have shown that the initially coherent liquid jet in supersonic crossflow breaks up or fractures at locations shortly behind the local sonic point along the jet column. Correlations by Li and Karagozian[22] show that the sonic point on the liquid jet is located farther downstream with "increasing momentum flux ratio and decreasing Mach number." According to these correlations, the jet injected into the Mach 2.5 boundary layer would fracture approximately three diameters sooner than the jet injected into the Mach 3.2 boundary layer for momentum flux ratios ranging between 5 and 8. However, this distance is very small and by itself cannot explain the relatively significant differences in the spreading of the two jets observed here.

The rapid acceleration of the mean flow at the Prandtl-Meyer corner augments both the lateral and vertical spreading of the upstream jet. As visualized by laser light scattering (Fig. 15), jet cross sections indicate that the lateral and vertical dimensions increase by nearly 100%. The apparent vertical spreading of the jet through the expansion is likely to be in part a consequence of the divergence of the streamlines through the expansion. It is also due in part to an inability of liquid droplets to follow the flow. However, these scenarios do not explain the relatively large *lateral* spreading of the jet close to the wall. As in the cross section of the downstream jet, the effect may be the result of strong streamwise vortices produced by an interaction of the jet and boundary layer and amplified by the rapid streamwise acceleration.

The streamwise growths of the jets measured from the laser cross sections are shown in Fig. 16. The ordinate in Fig. 16 denotes the maximum height of jet concentration at each streamwise location, examples of which are shown in Figs. 13-15. Here, the growths of the two jets are nearly equal up to $x/d = 28$ from their respective injection points. Thereafter, the upstream jet encounters the expansion fan, and its vertical penetration is almost doubled by the divergence of the streamlines and by the inability of larger droplets to follow the flow. Beyond about $70d$, this jet effectively ceases to grow. The downstream jet, on the other hand, has a weak growth between $30d$ and $80d$ and a more rapid growth thereafter. This rapid growth is probably because of the retransition of the partially laminarized boundary layer to a turbulent state.

Conclusions

Acetone was injected into a supersonic crossflow from a round orifice both upstream and downstream of a Prandtl-Meyer fan. The upstream jet was injected into a fully turbulent Mach 2.5 boundary layer at a jet-to-freestream momentum ratio of 0.92. The vertical and lateral dimensions of the cross section of the upstream jet were stretched nearly 100% as it negotiated the expansion fan. After the expansion fan, the vertical growth of the upstream jet was not significant. The downstream jet was injected into a highly accelerated, laminarized Mach 3.2 boundary layer at a jet-to-freestream momentum ratio of 0.92. The cross-sectional structure of this

jet was similar to its upstream counterpart except at locations near the wall below $y/d \sim 1$ where the lateral dimension of the jet was about twice as large. This difference may be the result of strong horseshoe vortices created by the relatively large near-wall velocity (and Mach number) gradients of the accelerated boundary layer interacting with the jet and upstream shocks. Wall flow patterns indicated that the separation zone of the downstream jet extended 4.7 diameters upstream of the jet exit compared with approximately 2.6 diameters for the upstream case. Schlieren pictures showed that the bow shock of the downstream jet was less detached than that of the upstream jet. Beyond $x/d = 80$, the downstream jet grew rapidly in the vertical direction. The rapid growth appears to be most likely due to the reversion of the partially laminarized boundary layer to a turbulent state.

Further work is required to quantify these interactions of jets and accelerated boundary-layer flows. A complete understanding of the different spreads of the jets injected upstream and downstream requires a more complete understanding of the interaction of the velocity fields of the jet and the boundary layer, especially during the acceleration.

Acknowledgment

This research was supported by a grant from the NASA Langley Research Center.

References

[1]Zukoski, E. E., and Spaid, F. W., "Secondary Injection of Gases into a Supersonic Flow," *AIAA Journal*, Vol. 2, No. 10, 1964, pp. 1689–1696.

[2]Kumar, A., Bushnell, D. M., and Hussaini, M. Y., "A Mixing Augmentation Technique for Hypervelocity Scramjets," AIAA Paper 87-1882, June 1987.

[3]Berman, H. A., Anderson, J. K., and Drummond, J. P., "Supersonic Flow over a Rearward Facing Step with Transverse Nonreacting Hydrogen Injection," *AIAA Journal*, Vol. 21, No. 12, 1983, pp. 1707–1713.

[4]Narasimha, R., and Sreenivasan, K. R., "Relaminarization in Highly Accelerated Turbulent Boundary Layers," *Journal of Fluid Mechanics*, Vol. 61, Pt. 3, 1973, pp. 417–447.

[5]Narasimha, R., and Viswanath, P. R., "Reverse Transition at an Expansion Corner in Supersonic Flow," *AIAA Journal*, Vol. 13, No. 5, 1975, pp. 693–695.

[6]Dussauge, J. P., and Gaviglio, J., "The Rapid Expansion of a Supersonic Turbulent Flow: Role of Bulk Dilatation," *Journal of Fluid Mechanics*, Vol. 174, Jan. 1987, pp. 81–112.

[7]Johnson, A. W., and Sreenivasan, K. R., "Laminarization and Retransition of Turbulent Boundary Layers in Supersonic Flow," *Bulletin of the American Physical Society*, Vol. 35, No. 10, 1990, p. 2314.

[8]Smith, D. R., and Smits, A. J., "The Rapid Expansion of a Turbulent Boundary Layer in a Supersonic Flow," *Theoretical and Computational Fluid Dynamics*, Vol. 2, No. 6, 1991, pp. 319–328.

[9]Shang, J. S., McMaster, D. L., Scaggs, N., and Buck, M., "Interaction of Jet in Hypersonic Cross Stream," *AIAA Journal*, Vol. 27, No. 3, 1989, pp. 323–329.

[10]Forde, J. M., Molder, S., and Szpiro, E. J., "Secondary Liquid Injection into a Supersonic Airstream," *Journal of Spacecraft and Rockets*, Vol. 3, No. 8, 1966, pp. 1172–1176.

[11]Heister, S. D., Nguyen, T. T., and Karagozian, A. R., "Modeling of Liquid Jets Injected Transversely into a Supersonic Crossflow," *AIAA Journal*, Vol. 27, No. 3, 1989, pp. 1727–1734.

[12]Allen, J. M., "Impact Probe Displacement in a Supersonic Turbulent Boundary Layer," *AIAA Journal*, Vol. 10, No. 4, 1972, pp. 555, 556.

[13]Kistler, A., "Fluctuation Measurements in a Supersonic Turbulent Boundary Layer," *Physics of Fluids*, Vol. 2, No. 3, 1959, pp. 290–296.

[14]Smits, A. J., and Muck, K. C., "Constant Temperature Hot-Wire Anemometer Practice in Supersonic Flows," *Experiments in Fluids*, Vol. 1, No. 1, 1983, pp. 83–92.

[15]Morkovin, M. V., "Effects of Compressibility on Turbulent Flows," *Mécanique de la Turbulence*, edited by A. Favre, Centre National de la Recherche Scientifique, Paris, 1962, pp. 367–380.

[16]Smith, M. W., "Flow Visualization in Supersonic Turbulent Boundary Layers," Ph.D. Thesis, Dept. of Mechanical and Aerospace Engineering, Princeton Univ., Princeton, NJ, 1989.

[17]Prasad, R. R., and Sreenivasan, K. R., "Scalar Interfaces in Digital Images of Turbulent Flows," *Experiments in Fluids*, Vol. 7, No. 4, 1989, pp. 259–264.

[18]Van Driest, E. R., "Turbulent Boundary Layer in Compressible Fluids," *Journal of Aeronautical Science*, Vol. 18, No. 3, 1951, pp. 145–160.

[19]Jayaram, M., Taylor, M. W., and Smits, A. J., "The Response of a Compressible Turbulent Boundary Layer to Short Regions of Concave Surface Curvature," *Journal of Fluid Mechanics*, Vol. 175, Feb. 1987, pp. 343–362.

[20]Zubkov, A. I., and Glagolev, A. I., "The Effect of Boundary Layer Thickness and Transverse Curvature of the Surface on the Geometry and Forces Acting in the Separation Zone Produced by Injection of a Jet into a Supersonic Flow over That Surface," *Fluid Mechanics-Soviet Research*, Vol. 8, No. 1, 1979, pp. 69–79.

[21]Hung, C.-M., and Buning, P. G., "Simulation of Blunt-Fin-Induced Shock-Wave and Turbulent Boundary-Layer Interaction," *Journal of Fluid Mechanics*, Vol. 154, May 1985, pp. 163–185.

[22]Li, H.-S., and Karagozian, A. R., "Breakup of a Liquid Jet in Supersonic Crossflow," *AIAA Journal*, Vol. 30, No. 7, 1992, pp. 1919–1921.